DISRUPTION DESIGN CRITERIA FOR JOINT EUROPEAN TORUS IN-VESSEL COMPONENTS

VALERIA T. G. RICCARDO,* PHILIP L. ANDREW, ALAN SANDFORD KAYE, and PETER NOLL
United Kingdom Atomic Energy Authority/Euratom Association, Culham Science Center
Abindgon, OX14 3DB, United Kingdom

Received February 4, 2002
Accepted for Publication October 1, 2002

In view of the modification to the Joint European Torus (JET) plasma facing components foreseen for the 2004 shutdown, the disruption design criteria for in-vessel components have been updated building on the operational experience with divertor plasmas gained since the early 1990s. In fast disruptions the largest contribution to the electromechanical loads comes from currents induced by the poloidal field change. This is proportional to the plasma current decay rate, the maximum of which is observed to be linear with the predisruption plasma current, as if the current quench in the fastest events has a fixed duration, around 10 ms. Usually vertical displacement events (VDEs) take place on a longer timescale. In these cases halo currents determine the worst loading condition. Analysis of recent VDE data confirmed the previously observed magnitude of asymmetries: toroidal peaking factor times ratio of average poloidal halo to initial plasma current up to 0.42.

Experimental evidence to justify the new criteria and procedures for applying them to JET are included. The revised design criteria are discussed and compared with those used for the components already present in the JET vessel.

KEYWORDS: *disruption, in-vessel components, halo current*

I. INTRODUCTION

Since disruptions are still to a large extent unavoidable and give rise to the highest loads on the Joint European Torus (JET) vacuum vessel and the in-vessel components, a realistic assessment of the worst-case loads is essential to the design of new in-vessel components.

*E-mail: valeria.riccardo@jet.uk

During vertical displacement events (VDEs) and disruptions, in-vessel conducting components experience electromechanical loads. These loads arise from the interaction of both induced currents and halo currents with the background magnetic field. Disruptions at JET can be divided into slow and fast in order to determine a reasonable, but still safe, combination of eddy and halo current loads for each component. Large plasma displacements at near full current have high halo current but are associated with slower current quenches, while rapid current quenches induce high eddy currents but are accompanied by less halo current. Therefore, these two load components can be at least partially decoupled.

The magnetic diagnostics used in this analysis are described in Sec. II. The categorization of disruptive events is substantiated by past experimental data in Sec. III of the paper. In Sec. IV high current quench events are analyzed in terms of poloidal field variation around the perimeter of the vessel. A discussion on global halo current parameters is presented in Sec. V, while in Sec. VI the assumptions of the halo current density and wetted area necessary to calculate electromechanical loads on in-vessel components are presented. The aim of this study is to provide a guideline for the assessment of disruption loads during the design phase of new in-vessel components; therefore, in Sec. VII the results presented in the paper are summarized and translated into usable recipes.

II. MAGNETIC DIAGNOSTICS

Only for a brief period of operation has JET had poloidal halo current diagnostics working in more than one toroidal location, and then only for upward (away from the divertor) events. The toroidal field pickup coils were fitted at the top of the vessel in octants 3 and 7 (180 deg apart, Fig. 1) when the MkI divertor was installed in 1993 (circa pulse 29 000). The one in octant 3 is still working, but the octant 7 probe failed during the disruption of pulse 39 055. There has been a toroidal

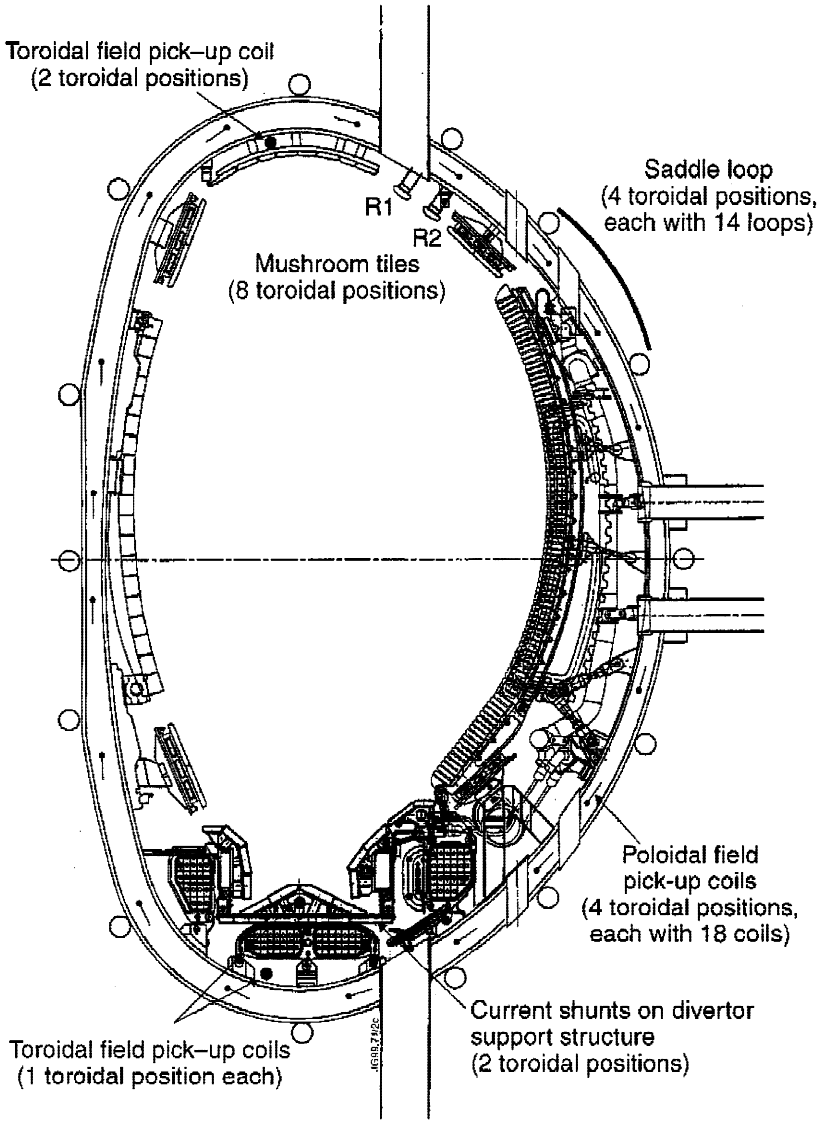

Fig. 1. Disruption relevant magnetic diagnostics.

field pickup coil at the bottom of the vessel during MkI. One above the divertor support structure was added when MkIIa was installed, and another one with MkII-GB. The probes above the divertor support structure measure the current flowing in both the structure and the bottom of the vessel, while the probe below the divertor support structure yields the current flowing in the bottom of the vessel.

With the MkII-GB magnetic configuration, almost all disruptions went upward. Therefore, the analysis of halo asymmetries for downward disruptions is based on MkIIa data from shunts fitted poloidally across the continuous metallic MkII structure that supports the divertor. The halo current data discussed in this paper are mostly taken from MkI (upward only) and MkIIa (upward and downward) disruptions. The history of the JET toroidal field pickup coils is summarized in Table I, while a detailed description of the halo diagnostic system (including the mushroom tiles) at the time when the data were obtained can be found in Ref. 1.

TABLE I

History of Availability of Toroidal Field Pickup Coils

	Pulse Range
Top 3	29 000 to now
Top 7	29 000 to 39 000
Bottom 3 (below MkII)	29 000 to 43 000
Bottom 4 (above MkII)	36 000 to 52 000
Bottom 8 (above MkII)	44 000 to now

Apart from halo specific diagnostics, in each of the JET vessel octants, there is an array of 18 poloidal field pickup coils just inside the inner shell and an array of 14 saddle loops just outside the outer shell (Fig. 1). In addition, the poloidal field parallel and perpendicular to the divertor support structure is measured in two toroidal locations (11 pairs of pickup coils each, octants 2 and 6), and three arrays of pickup coils measure the field parallel to the outer poloidal limiter.

III. CATEGORIES OF DISRUPTIONS

The toroidal field pickup coils act as segments of a toroidal Rogowski coil to estimate the poloidal component of the halo current. The poloidal halo current is then estimated assuming toroidal uniformity. We define the halo current fraction as the maximum of the ratio of the average poloidal halo current to the plasma current just before the disruption; the average is between the two pickup coil measurements for upward events and between the two poloidal shunt measurements for downward events. The toroidal peaking factor (TPF) is defined as the ratio between the peak and the average halo current. No current reversal has been observed at the toroidal field pickup coils, and typical JET values for the TPF are 1 to 2. Assuming the halo current pattern has $n = 1$, the TPF can be underestimated by up to 50% by two probes 180 deg apart. Both the halo current fraction (Fig. 2) and the TPF (Fig. 3) increase at lower plasma current quench rate. The maximum observed halo fraction during upward events (0.23) is smaller than that observed in downward events (0.36); the largest observed TPF is 2 in upward events and 1.34 in downward events. As halo currents cause vessel forces, and hence

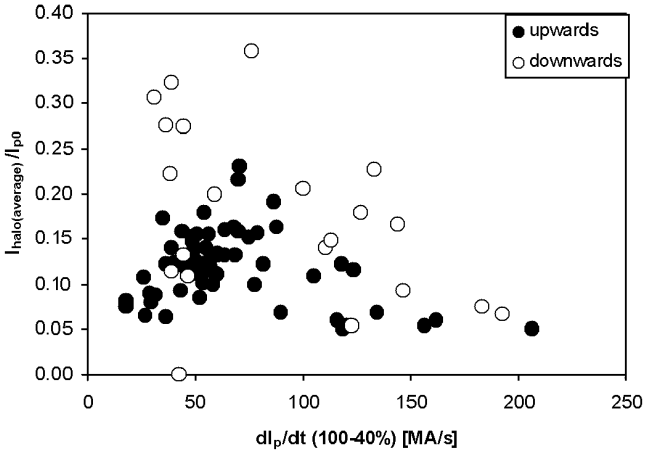

Fig. 2. The ratio average poloidal halo current to initial plasma current peaks at low current quench rate; data from JET MkI and MkIIa operation.

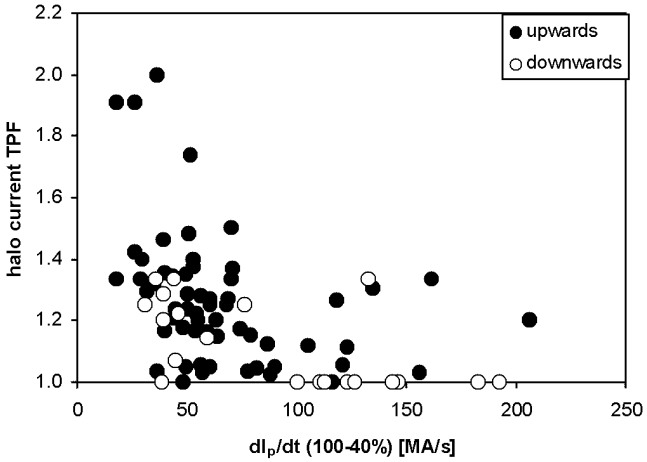

Fig. 3. The TPF peaks at low current quench rate.

displacements, these forces and displacements are an indirect, but more easily available, measure of the magnitude and asymmetry of disruption electromechanical loads. The vessel sideways displacements, which are closely linked to plasma and halo asymmetries,[2] are only substantial (1 to 7 mm) after events with slow plasma current quench rate ($<30\ s^{-1}$), as illustrated in Fig. 4. This confirms for a larger number of events the results of Fig. 3: Plasma asymmetries are present for only rather slow events. Therefore, the loads induced by eddy currents in fast plasma current quench and by high and strongly localized halo current in slow events can be studied separately and combined with weight factors smaller than unity.

Already in DIII-D (Ref. 3) disruptions have been divided into major (fast) disruptions and (slow) VDEs, based on a theory[4] that describes the behavior of boundary safety factor, current decay rate, and vertical position

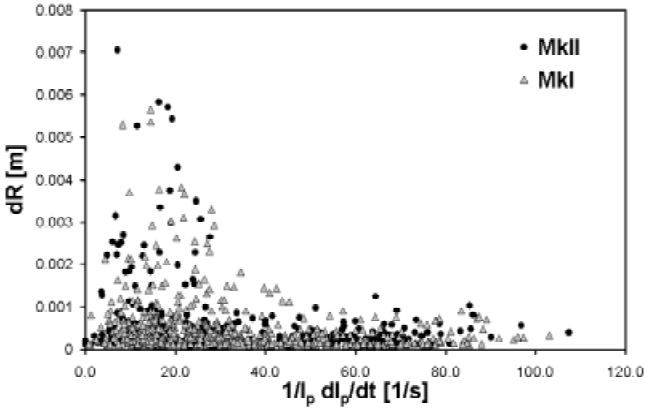

Fig. 4. The largest vessel sideways displacements occur only after relatively slow disruptive events.

instability growth rate. A similar dependence on the plasma current quench time is seen in the Asdex Upgrade for asymmetries[5] and less clearly for the halo current fraction.[6]

The reason why asymmetries appear mainly in the slowest events is that only in these can the boundary safety factor decrease to the critical value of ~1 at which kink instabilities are triggered. In fast disruptions, the current quenches too quickly for the plasma to reach a large displacement at a significant fraction of the initial current, and hence for the boundary safety factor to decrease to its critical value. The same argument can be used to justify the existence of a link between slow disruptions and large halo current fraction. While the halo current provides most of the vertical plasma force balance in slow disruptions, it is of minor importance in faster disruptions where the observed increase of the vertical plasma current moment is relatively small. This is in contrast with other tokamaks, notably COMPASS and Alcator C-mode, where the halo current is thought[7] and measured[8] to be mainly linked to the peak instantaneous plasma current quench rate, and hence larger in faster events, or the vertical displacement speed.[9]

IV. FAST DISRUPTIONS

During fast plasma current quench disruptions (typically shorter than 30 ms at JET), the dominant source of electromechanical loads on in-vessel components is the eddy current induced by the poloidal field variation. Data from disruptions of diverted plasmas (MkI and MkIIa) show that the envelope of the plasma current quench rate is linear with the initial plasma current (Fig. 5), as if the minimum duration of disruptions (~10 ms) does not depend on the initial current. Thus, in fast disruptions, the maximum poloidal field rate of change is proportional to the plasma current, and the eddy current loads from past operational data can be scaled to predict those that would occur as a consequence of a disruption at the higher design plasma current level.

The rate of change of the poloidal field parallel to the vessel wall (Fig. 6) depends both on the plasma displacement velocity and on the plasma current quench rate. At the top of the vessel, the field variation is dominated by the plasma displacement rather than by the current decay. In fact the parallel field rate of change reaches the largest values at low quench rate, which is typical of VDEs. The probes at the top of the vessel are located very close to the boundaries of the plasma region and are only weakly screened by the conductive but toroidally segmented structure of the dump-plate below them. Consequently, at the vessel midplane the field variation is dominated by the current quench and increases monotonically with it. The bottom of the vessel is effectively screened from fast field transients by the toroidally continuous conductive divertor structure. The variation of the field perpendicular to the vessel wall (Fig. 7) behaves similarly to that of the parallel field at the top and the inner midplane of the vessel, less so at the outer midplane. It is smaller both because the radial field itself is smaller and because the vessel shell partially screens its transient.

The variation of the poloidal field parallel to the poloidal limiter (Fig. 8) is larger than that at the outer wall (Fig. 6), as it is closer to the plasma. At the divertor structure the poloidal field variation is smaller than at the top of the vessel and less dependent on the current quench. This is again because the support structure, in which the probes are fitted, acts as a filter.

To estimate the field variation in regions where no magnetic diagnostics are available (e.g., radial field on the outer poloidal limiter), transient calculations imposing the measured poloidal field coil currents and the

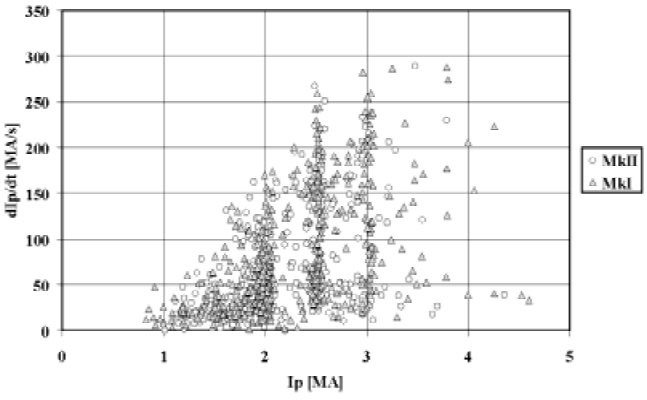

Fig. 5. The upper envelope of the plasma current quench rate (100 to 40%) is linear with the initial plasma current.

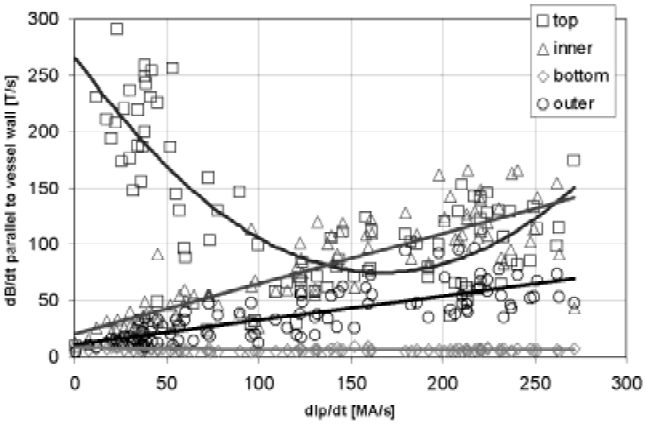

Fig. 6. Peak time derivative of the poloidal field parallel to the vessel wall as a function of the 100 to 40% plasma current quench rate (MkIIa and MkII-GB upward disruptions with plasma current between 3 and 4 MA).

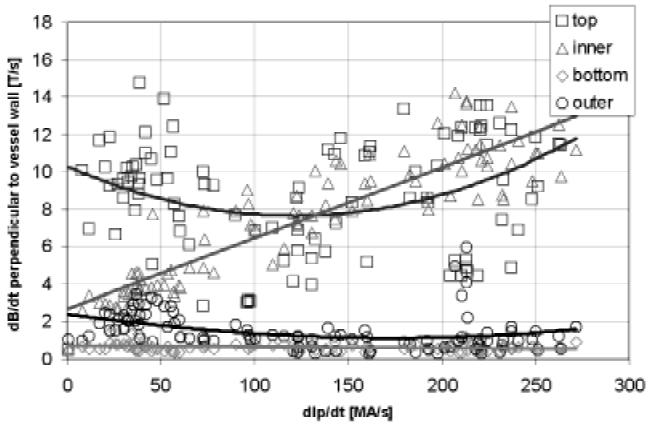

Fig. 7. Peak time derivative of the poloidal field perpendicular to the vessel wall as a function of the 100 to 40% plasma current quench rate (same database as Fig. 6).

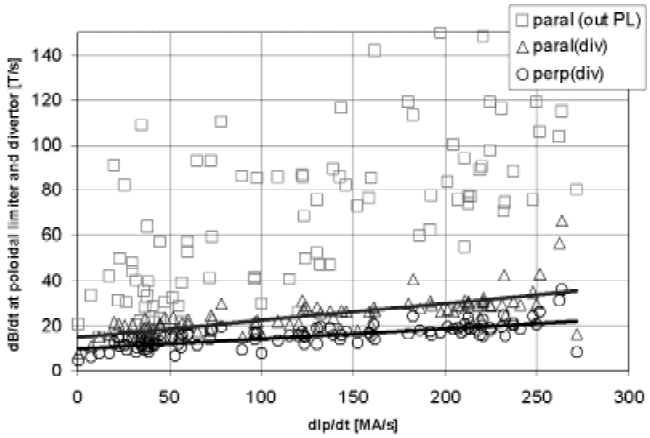

Fig. 8. Peak time derivative of the poloidal field at the outer poloidal limiter and divertor as a function of the 100 to 40% plasma current quench rate (same database as Fig. 6).

plasma current and position have been carried out with MaxFEA (Ref. 10). The poloidal field rate of change calculated for the actual disruption has been scaled to the design plasma current (6 MA), which includes a margin on the actual plasma current levels planned for the near future operation, assuming these vary linearly with the predisruption plasma current. This is a pessimistic assumption as some extreme configurations can be run only at a rather low level of plasma current, due to limitations in the poloidal field coil currents and to avoid excessive out-of-plane forces on the toroidal field coils. As a combined result of the data analysis and the disruption simulation, the design values of Table II have been obtained. These are the same as the original design values at the divertor and slightly lower at the outer poloidal limiter

TABLE II

Design Values for the Poloidal Field and Its Time Derivative

	Parallel		Perpendicular	
	(T)	(T/s)	(T)	(T/s)
Divertor	1	100	1	100
Poloidal limiter	1.2	120	0.4	80
Wall (inner)	1.2	250	0.4	30
Wall (outer)	1.2	70	0.4	10
Wall (top)	1.2	350	0.4	20
Wall (bottom)	1.2	30	0.4	10

(originally, they were 150 and 120 T/s for parallel and perpendicular components, respectively).

V. GLOBAL HALO PARAMETERS

The ratio of average poloidal halo current to predisruption plasma current f and the TPF used in Figs. 2 and 3 (to show that the worst events in terms of halo current are those at low plasma current quench rate) are now plotted against each other in Fig. 9. The (f, TPF) space covered by JET data is within the multimachine scatter used as the ITER reference[11]: Most events stay below $f \cdot \mathrm{TPF} = 0.42$ (which has been set as the JET design criteria), and all of them are below $f \cdot \mathrm{TPF} = 0.5$ (the ITER design value).

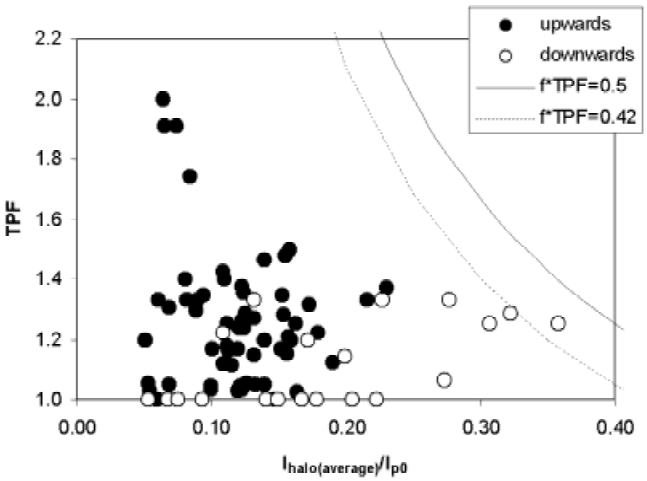

Fig. 9. TPF and ratio average poloidal halo current to initial plasma current.

The maximum value of both the ratio of average poloidal halo current to initial plasma current (Fig. 10) and the halo current TPF (Fig. 11) are increased when the minimum boundary safety factor during the disruption decreases below 2. The definition of the boundary safety factor used here is for a low poloidal beta β_p and large aspect ratio plasma. Given the plasma position (R_p, z_p) and assuming a plasma elongation k of 1.5 (smaller than the typical equilibrium elongation, as discussed in Ref. 12), the minimum distance of the plasma center from the wall, and therefore the plasma minor radius a_p, can be determined. The boundary safety factor can therefore be estimated during the disruption as

$$q = \frac{B_T a_p^2 \pi}{\mu_0 I_p R_p} (1 + k^2) \ , \qquad (1)$$

where B_T is the toroidal field at the plasma center. The resulting boundary safety factor is usually in good agreement with the last converged points (just before the disruption) of the EFIT (Ref. 13) reconstruction.

The boundary safety factor is particularly significant for asymmetries leading to vessel sideways displacements, as these seem to be triggered only when the boundary safety factor decreases below a critical value of ~1 during the disruption.[12] Since the divertor coils and structure have been installed in the bottom part of the JET vacuum vessel, only VDEs going upward have made the torus move sideways. This is consistent with the measured halo TPF for the set of events analyzed here. In Fig. 11 the highest TPFs are observed in upward events.[12]

The average poloidal halo current is proportional to the variation in plasma vertical current moment (Fig. 12). Here, the upward and the downward events lie on different lines because of the attraction between plasma current and divertor coil currents, requiring more halo current for the plasma force balance of downward events. The largest variations in plasma vertical current moment are reached during slow VDEs, when the plasma displaces significantly from the original vertical equilibrium position while losing only a small fraction of the starting current. In contrast, in fast disruptions most of the current is lost before the plasma has significantly displaced. This is consistent with the main role of the halo current being to provide the force balance for the plasma, for which the main destabilizing force is due to the departure from the original equilibrium position. Therefore, less demanding TPF and f can be assumed for components located near the midplane, which are likely to be wetted only during events with low plasma vertical

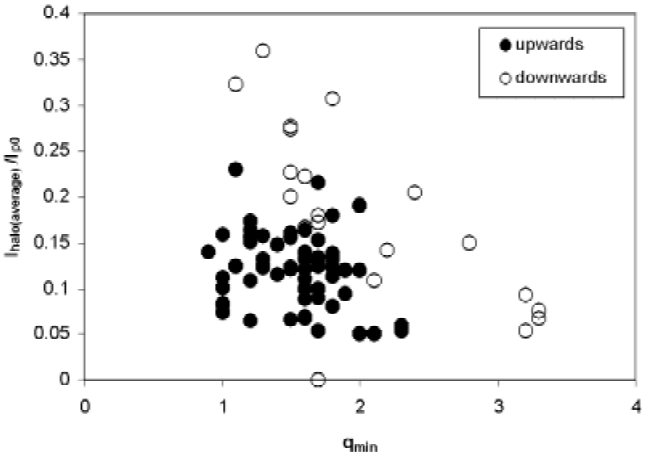

Fig. 10. Ratio average poloidal halo current to initial plasma current plotted versus the minimum boundary safety factor reached during the disruption.

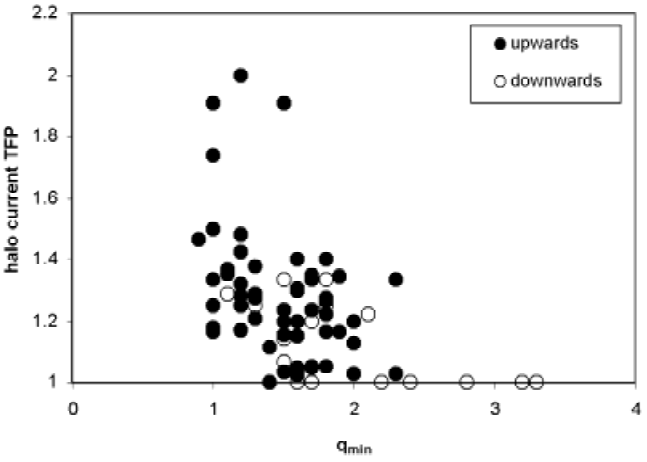

Fig. 11. TPF plotted versus the minimum boundary safety factor reached during the disruption.

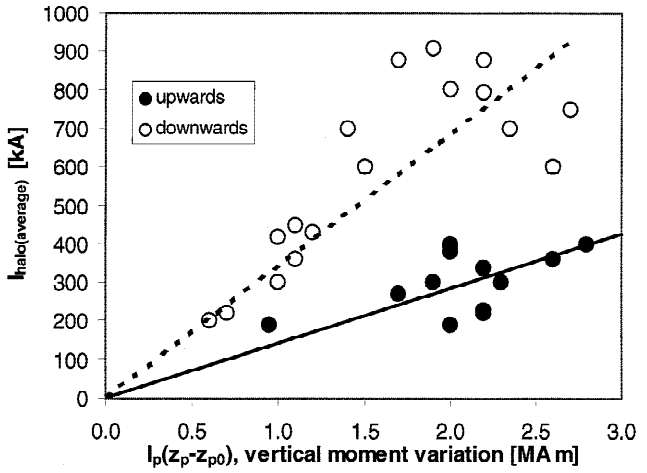

Fig. 12. Ratio average poloidal halo current to initial plasma current plotted versus the peak variation of the plasma vertical current moment.

displacement. On the contrary, larger peak halo current (TPF$\cdot f$) has to be assumed at the top and bottom of the vessel. The values of TPF and f chosen as design reference following the analysis of MkI and MkIIa disruptions are listed in Table III. Values of 20% for the halo fraction and 1.5 for the TPF have been generally used in the past.

VI. HALO CURRENT INTERCEPTION LOADS

In order to estimate the loads on in-vessel components, it is necessary to know the halo current density and the extent of the wetted poloidal arc. At JET these quantities cannot yet be measured accurately. The mushroom tiles have been used to estimate the halo current density.[14] The limitation of such a diagnostic is that it is located too far outboard to be wetted at the time the of the maximum halo current. The measurements at the mushroom tiles during a 3-MA disruption[14] indicate that the parallel halo current density is $\sim$1 MA/m^2. The halo current width along the local minor radius was estimated to be 0.08 m, which is consistent with the values discussed below (Table IV), given that the halo current had not reached its maximum when intercepting the mushroom tiles.

The halo current density and the extent of the wetted poloidal arc can be estimated if some, generally conservative, assumptions are made. For a plasma with flat current profile, which is reasonable as the energy quench is likely to have occurred already, expression (1) for the boundary safety factor can be rewritten as

$$j_T = \frac{B_T}{\mu_0 R_p}\,\frac{1}{q_{flat}}\,\frac{1+k^2}{k}\ , \tag{2}$$

to yield the toroidal current density j_T. Therefore, for a given toroidal field, the current density depends mainly on q_{flat} and only weakly on the plasma elongation [usually taken as 1.5 (Ref. 12)].

If the plasma current and radial position are given, the plasma minor radius and the poloidal halo current density can be calculated. For a $\beta_p = 0$ plasma (as it is reasonable to assume after the energy quench), the toroidal and poloidal current density j_P are linked:

TABLE III

Design Halo Current Parameters

	TPF	$f = I_{h(average)}/I_{p0}$	TPF$\cdot f$
Top	1.8	0.23	0.42
Bottom	1.4	0.30	0.42
Midplane	1.2	0.25	0.30

TABLE IV

Estimates of Halo Thickness at the Plasma Midplane

I_p (MA)	I_h (MA)	Minor Radius, a_p (m)	Halo Thickness, d_{mid} (m)
6.00	1.80	0.64	0.10
3.00	1.80	0.46	0.14
4.00	1.80	0.53	0.12
2.56	1.15	0.42	0.10
1.44	0.65	0.32	0.07

$$j_P/j_T = B_P/B_T\ . \tag{3}$$

Assuming conservatively (this leads to the smallest wetted arc and the highest local loads) that the halo current density is flat, the continuity of the poloidal halo current along the plasma poloidal perimeter implies that

$$I_h = 2\pi R_p\, d(\theta) j_P(\theta) \tag{4}$$

for any θ and independently of the elongation k. In expression (4) $d(\theta)$ is the halo thickness at the poloidal angle θ. This is not uniform along the plasma perimeter as the poloidal field also varies. At the plasma midplane, where

$$B_P/B_T = (ka_p)/(q_{flat} R)\ , \tag{5}$$

the halo thickness can be derived from expressions (3) and (4):

$$d_{mid} = \frac{I_h\, q_{flat}}{2\pi k a_p\, j_T}\ . \tag{6}$$

As an example the estimates of the halo thickness on the plasma midplane for a displaced plasma in contact with the divertor ($R_p \sim 2.6$ m) are reported in Table IV, imposing a toroidal field of $B_T = 4$ T (at $R_{ref} = 2.96$ m) and a boundary safety factor of $q_{flat} = 1$. The first column of Table IV is the plasma current when the plasma is just in contact with the divertor. The second column of Table IV is the assumed halo current at the time of the contact, as extrapolated from past operational observations. The plasma minor radius (third column, including both the core and the halo) is derived from

$$I_p = \pi k j_T a_p^2\ , \tag{7}$$

where j_T is a function of the elongation (typically assumed 1.5) and the boundary safety factor. The thickness of the halo region at the plasma midplane (fourth column in Table IV) is then derived from Eq. (6). When a TPF >1 has to be taken into account, the wetted footprint is increased as to maintain the poloidal halo current density constant and equal to the toroidally uniform case (4).

The first row of Table IV represents the direct application of the JET design criteria (6-MA plasma with a halo fraction of 30% in a downward event). This gives a rather large plasma (not compatible with the size of the divertor throat) and a relatively thin halo region. If the plasma current at the contact time is decreased while keeping constant the halo current at its design value, second and third row, the plasma size decreases, so the plasma can enter the divertor throat, and at the same time, the volume fraction occupied by the halo increases. The last three rows of Table IV simply show a plasma shrinking at constant halo fraction.

The divertor worst loading case may not occur at the time of the highest values of halo current, as at that stage the plasma may be still too large to enter the divertor throat. In the case sketched in Fig. 13, while the top tiles of the divertor are in contact with the halo channel of the main chamber (points A and H), the other tiles are shadowed. The tiles in the medium grey region may be subject to halo-like load due to a current driven by the voltage differential between the inner and the outer carriers. It is unlikely that the tiles in the lightest grey region see any halo current as the connection path is too short for this driven current to be supported.

However, for the sake of argument, if the same current density was present in the annular region inside the throat of the divertor (B-C to F-G) as on the upper leg of the halo flux tube (H to A), this current would have to be collected from the one intercepted in the top part of the divertor. In most cases this would lead to a force pushing the tile toward the carrier, which is not the most structurally challenging loading condition. Furthermore, this leg of the halo current path would not provide the required contribution to the global force balance on the vessel.

VII. DISCUSSION AND CONCLUSION

As far as electromechanical loads on in-vessel components are concerned, JET disruptions can be divided according to the speed of the plasma current quench. In fast events, loads are predominately due to eddy currents, while in slow events they are due to halo currents. Maps of the peak poloidal field rate of change, the halo current fraction, and the TPF have been obtained from past operational experience.

The eddy current and halo current loads usually have to be combined:

1. For slow disruptions the typical current quench time in JET VDEs is >30 ms, compared with the minimum quench time of ~ 10 ms. The poloidal field time derivative is less than half the worst case one, and for design purposes, 40% of the worst case eddy load should be combined with the full halo current load. However, due to the strong dependence on the plasma vertical displacement, the full eddy current load should be applied at the top of the vessel.

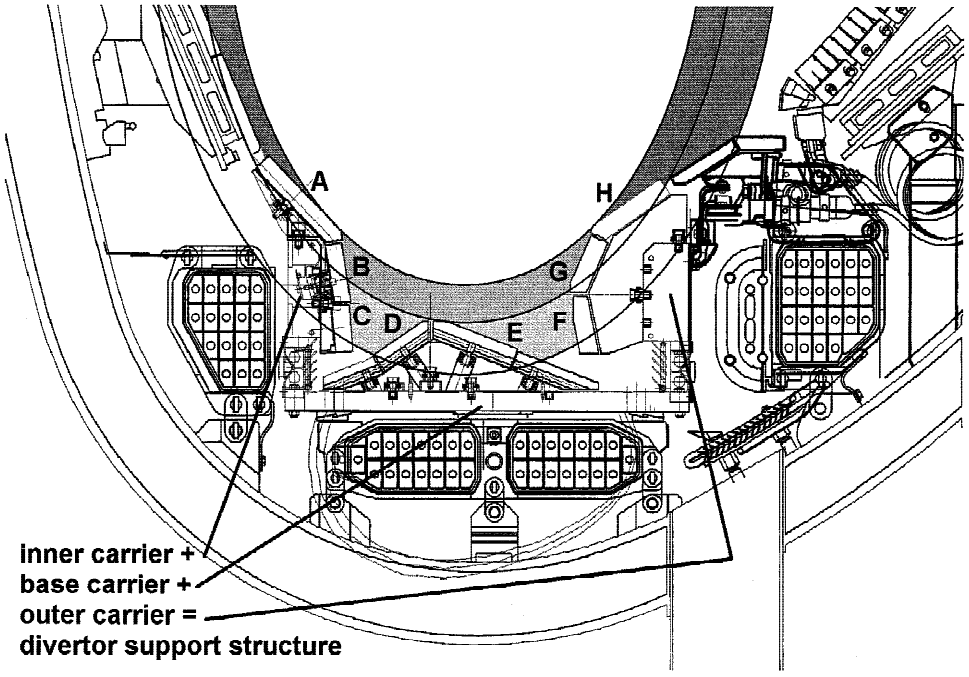

Fig. 13. Halo current intercepted by the divertor.

2. In fast disruptions the ratio of the average poloidal halo current to the starting plasma current is less than half that observed in VDEs; for design purposes, 40% of the worst-case halo load should be combined with the full eddy current load.

In most cases the halo dominated loading case is the more demanding. Weighted contribution of eddy and halo currents to the electromechanical loads applies to any tokamak, but the weights indicated here are JET specific.

Since small in-vessel components are generally wetted only by a fraction of the halo current (i.e., they cover a poloidal arc smaller than the halo footprint), some assumptions on the halo current density and width need to be done in order to define the relevant halo loads. As an example only the top tiles of a divertor shaped as the one in Fig. 13 would get the full halo flux tube of a typical JET disrupting plasma. However, some tiles further down in the divertor throat could experience electromechanical loads more challenging from the structural point of view even if the total amount of halo current they collect is less than that collected by the top tiles. Thus, when the collected current is constrained (by electrical boundary conditions) to flow in the direction opposite to the one it would have had in the plasma, a pulling force is exerted on the component, which applies bending stress to the tile supports. Another electrical constraint that enhances halo current loads is a poloidally distant grounding point, as this forces the current to travel a long way across the toroidal field. Therefore, not only the total amount of intercepted halo current but also the electrical boundary conditions determine the disruptive loads acting on in-vessel components. Furthermore, for components with a short toroidal extension that are intercepting the halo flux tube, it is important to account for not only the halo current entering from the front face but also that intercepted by the exposed side. Here, in fact, the current density is higher (since the toroidal field is larger than the poloidal field), and often the total current collected on the side is larger than that collected at the front.

Although the halo current diagnostic system at JET delivers only sparse data, the available information on both halo current and poloidal field transients helps in the design phase of new components, by allowing designing close to the structural limits. The new design requirements are more conservative on halo current and slightly more relaxed on eddy currents than those used in the past. This change is based on operational experience; for new machines, larger safety factors need to be used in order to account for the uncertainties in the predicted loads.

ACKNOWLEDGMENTS

We would like to thank C. Portafaix, P. Chappuis, and F. Durodie for their questions and C. Lowry for his comments.

This work has been conducted under the European Fusion Development Agreement and is partly funded by Euratom and the U.K. Department of Trade and Industry.

REFERENCES

1. P. ANDREW, P. NOLL, and V. RICCARDO, "The Relation Between Halo Currents and Plasma Displacement/Deformation in JET," *Proc. 17th Symp. Fusion Engineering*, p. 108, Institute of Electrical and Electronics Engineers/Nuclear and Plasma Sciences Society (1997).

2. V. RICCARDO, P. NOLL, and S. P. WALKER, "Forces Between Plasma, Vessel and TF Coils During AVDEs at JET," *Nucl. Fusion*, **40**, 1805 (2000).

3. A. G. KELLMAN et al., "Disruption Studies in DIII-D," *Proc. 16th Int. Conf. Fusion Energy*, Montreal, Canada, October 7–11, 1996, International Atomic Energy Agency (1996).

4. D. HUMPHREYS and A. G. KELLMAN, "Analytical Modeling of Axisymmetric Disruption Halo Currents," *Phys. Plasmas*, **6**, 2742 (1999).

5. G. PAUTASSO et al., "About Asymmetries of the Halo Current and Role of $q(\psi)$," presented at ITER Expert Group Workshop on MHD, Madeira, Portugal, June 25–26, 2001.

6. G. PAUTASSO, Personal Communication.

7. P. KNIGHT et al., "Analysis of Vertical Displacement Events and Halo Current in COMPASS-D," *Nucl. Fusion*, **40**, 325 (2000).

8. R. S. GRANETZ, "Disruptions and Halo Currents in Alcator C-Mod," *Nucl. Fusion*, **36**, 545 (1996).

9. Y. NEYATANI et al., "Characteristics of Halo Currents in JT-60U," *Nucl. Fusion*, **39**, 559 (1999).

10. P. BARABASCHI, "The MaxFEA Code," presented at Plasma Control Technical Mtg., Naka, Japan, April 1993.

11. "ITER Physics Expert Group on Disruptions, Plasma Control and MHD," ITER Physics Basis Eds., *Nucl. Fusion*, **39**, 2344 (1999).

12. V. RICCARDO, S. WALKER, and P. NOLL, "Parametric Analysis of Asymmetric Vertical Displacement Events at JET," *Plasma Phys. Controlled Fusion*, **42**, 29 (2000).

13. D. P. O'BRIEN et al., "Equilibrium Analysis of Iron Core Tokamaks Using a Full Domain Method," *Nucl. Fusion*, **32**, 1351 (1992).

14. P. ANDREW, P. MIELE, P. NOLL, R. PEARCE, M. PICK, and L. ROSSI, "Measured Currents in JET Limiters During Disruptions," *Proc. 16th Symp. Fusion Engineering*, p. 770, Institute of Electrical and Electronics Engineers/Nuclear and Plasma Sciences Society (1995).

Valeria T. G. Riccardo (Laurea, nuclear engineering, Politecnico di Torino, Italy, 1995; PhD, mechanical engineering, Imperial College, London, United Kingdom, 1998) is currently engineering analysis group leader at the Joint European Torus (JET) Facility, Culham Laboratory. Her current responsibility is scientific support to the JET chief engineer. Her current research interest is magnetic fusion including disruptions and in-vessel component design.

Philip L. Andrew (BSc, engineering physics, Queen's University, Canada, 1986; PhD, applied physics, University of Toronto, Canada, 1991) is currently an experimental physicist at the JET Facility, Culham Laboratory. His current responsibilities include JET infrared thermograph diagnostics. His current research interest is magnetic fusion, including disruptions and power load to the first wall.

Alan Sanford Kaye (BSc, physics, Australian National University, 1964; DPhil, plasma physics, Oxford University, United Kingdom, 1968) is the chief engineer at the JET Facility, Culham Laboratory. He is responsible for design standards and operating limits of the JET tokamak and for implementation of enhancements on JET. His current interests are tokamak engineering and radio-frequency heating systems.

Peter Noll (Dipl Ing, 1954, and Dr rer nat, physics, 1960, Technische Hochschule, Munich, Germany) is currently retired.